JOURNAL OF SOLID STATE CHEMISTRY 103, 16–24 (1993)

Correlation between Vibrational Spectrometry Behavior and Oxidation Mechanism of Molybdenum Substituted Magnetites

B. DOMENICHINI AND B. GILLOT

Laboratoire de Recherche sur la Réactivité des Solides, URA 23 CNRS, Faculté des Sciences Mirande, B.P. 138, 21004 Dijon Cedex, France

AND L. BOUET, P. TAILHADES, AND A. ROUSSET

Laboratoire de Chimie des Matériaux Inorganiques, URA 1311 CNRS, Université Paul Sabatier, 118, route de Narbonne, 31062 Toulouse Cedex, France

Received March 12, 1992; in revised form June 26, 1992; accepted July 6, 1992

The oxidation behavior of molybdenum substituted magnetites, $Fe_{3-x}Mo_xO_4$, has been investigated by Fourier transform infrared transmission. When the oxidation of Fe^{2+}, Mo^{3+}, and Mo^{4+} ions is achieved below 530°C, optical spectroscopy confirms the formation of cation-deficient spinels with a vacancy and cation ordering that depends on both oxidation and molybdenum content. The intense band at 840 cm^{-1} observed for cation-deficient spinels, as well as for transformation products, and the disappearance of the band at 726 cm^{-1} for initial samples prove that Mo^{6+} ions are present at tetrahedral sites of the spinel lattice. However, under certain thermal treatments, the Mo^{6+} ions remain in octahedral sites, namely when the octahedral sites are also occupied by Fe^{2+} ions.

Introduction

In previous investigations (*1–3*) we have determined by derivative thermogravimetry the cation distribution and oxidation mechanism of molybdenum-substituted magnetites, $Mo_{3-x}Fe_xO_4$, prepared by precipitation methods. These lead to submicrometer molybdenum ferrites (*1*) with $0 < x < 0.63$; by a standard ceramic route for molybdenum substitution one obtains samples with $0 < x < 1$ (*2*). From these studies it is concluded that the submicrometer molybdenum ferrites can be represented by the ionic configuration:

$$(Mo^{4+}_{\gamma x}\ Fe^{3+}_{1-\beta-\gamma x}\ Fe^{2+}_{\beta})_A\ (Mo^{3+}_{(1-\alpha)x}\ Mo^{4+}_{(\alpha-\gamma)x}\ Fe^{3+}_{1+\beta-(1+\alpha-\gamma)x}\ Fe^{2+}_{1-\beta+\alpha x})_B\ O^{2-}_4 \quad (1)$$

with $\alpha = 0.11$, $\gamma = 0.01$, and β increasing with x. The subscripts A and B refer, respectively, to occupancy of tetrahedral and octahedral sites of the spinel structure. For molybdenum ferrites prepared by the ceramic route, the cationic distribution depends on

0022-4596/93 $5.00

grinding time; the presence of Mo^{4+} ions at tetrahedral sites has not been detected (*2*).

Whatever the preparation method, these mixed oxides contain several oxidizable cations (Fe^{2+}, Mo^{3+}, Mo^{4+}) distributed on both *A* and *B* sites of the spinel structure. For temperatures below about 500°C, cation-deficient spinels associated with a large number of vacancies are obtained; these are generated by the following reaction chain (*3*):

$3Fe_B^{2+} \rightarrow 2Fe^{3+} + \square$

oxidation temperature peak 200°C

$2Mo_B^{3+} \rightarrow Mo^{6+} + \square$

oxidation temperature peak 300°C

$3Mo_B^{4+} \rightarrow 2Mo^{6+} + \square$

oxidation temperature peak 385°C

$3Fe_A^{2+} \rightarrow 2Fe^{3+} + \square$

oxidation temperature peak 420°C

$3Mo_A^{4+} \rightarrow 2Mo^{6+} + \square$

oxidation temperature peak 490°C

Our thermogravimetric data provide more information on the cation distribution than previous studies via electrical properties and Mössbauer analyses (*4*, *5*). The α, β, γ coefficients have been accurately determined and the presence of Mo^{4+} ions in *A* sites has been proved. However, the possibility of an ordered distribution of cations and vacancies at *B* sites and an eventual migration of cations between *A* and *B* sites during the oxidation process has not been adequately specified by the techniques employed.

To complement the physicochemical characterization of the new mixed oxides as catalysts (*6*), we have attempted to establish correlations between the structural and vibrational properties by correlating the oxidation state of molybdenum and the vacancy content with the cation distributions induced by the selective oxidation reactions.

Experimental

Samples

The molybdenum ferrites, $Mo_xFe_{3-x}O_4$, were prepared in two ways:

(i) by precipitation of Fe^{2+}, Fe^{3+}, and Mo^{5+} chloride solutions in alkaline medium (samples A). A thermal treatment of these mixed oxides under N_2–H_2–H_2O mixture between 400 and 800°C leads to solid solutions $Fe_3O_{4(1-x)}Fe_2MoO_{4(x)}$ with $0 < x < 0.63$. The crystallite size close to 50 nm renders them highly reactive with oxygen. A first structural investigation was undertaken, based on the variation of lattice parameters with x and on calorimetric and thermogravimetric analyses of oxidized samples (*1*, *3*). For starting samples, the distribution can be formulated as Eq. (1), in recognition of the strong octahedral site preference of Mo^{3+} and Mo^{4+} ions (*5*).

(ii) by mixing in an agate mortar powders of Fe, Fe_2O_3, and MoO_2 in appropriate molar ratios with different values of x ($0 < x < 1$, samples B) (*2*). The homogenized powder was put into an alumina crucible placed inside a silica ampoule. The amoule was then degassed under vacuum (10^{-4} Pa) to avoid oxidation at high temperature, sealed, and heated at 1150°C for 3hr, after which it was quenched in water. The samples were analyzed by X-ray diffraction and were found to be a single-phase cubic spinel structure. The lattice parameter increased monotonically from 0.8398 ($x = 0$) to 0.8512 nm ($x = 1$). Such treatment at high temperature causes an increase of the crystallite size; the average diameter observed from electron microscopy was on the order of 2 to 3 μm. $Fe_2Mo_3O_8$ and $Fe_2(MoO_4)_3$ were prepared in the same way, respectively at 1160°C under vacuum and at 800°C in air.

Measurements

The oxidation were performed under isothermal conditions or with the temperature increasing at a linear rate (2.5°C min^{-1}) in a Setaram MT-B 10-8 microbalance using 6 mg of initial powder (sample A) or ground powder (sample B). The degree of oxidation of the samples at various levels of reaction was calculated from the gravimetric data.

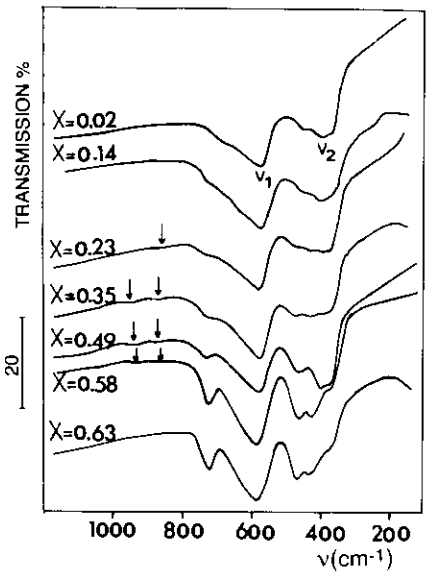

FIG 1. FT-IR spectra of A samples for $0 < x < 0.63$.

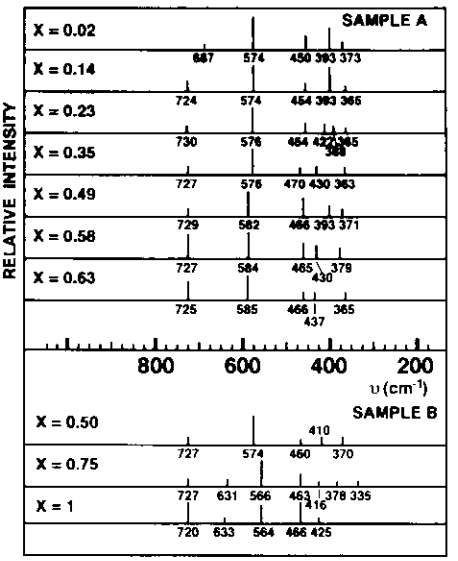

FIG. 2. Vibrational behavior of $Fe_{3-x}Mo_xO_4$ spinels for A and B samples.

The IR spectra were recorded with a Perkin–Elmer 1725X FT-IR spectrometer over the range 4000–450 cm^{-1} and with a Perkin–Elmer 1700X FT-IR (Fourier transform IR) spectrophotometer over the range 450–50 cm^{-1}. About 1 mg of sample was mixed with 200 mg of spectroscopically pure dry CsI or with 50 mg of polyethylene and pressed into rods before the spectrum was recorded.

Results

Initial Phases

Representative IR spectra from 1200 to 150 cm^{-1} for samples A with $0.02 < x < 0.63$ are depicted in Fig. 1 and the positions of the IR bands are shown in Fig. 2. For composition range $0 < x < 0.49$ the spectra reveal two strong absorption bands, ν_1 and ν_2, which for $x = 0.02$ occur at 574 and 393 cm^{-1} and for $x = 0.49$ at 582 and 393 cm^{-1}. For the highest concentration of molybdenum and samples B with $x > 0.50$ (Fig. 3), the band at about 390 cm^{-1} progressively disappears.

Close to 440 cm^{-1}, two small bands with low intensity appear for certain concentrations of molybdenum. At the lowest concentrations these bands are not seen clearly, but their intensity increases with concentration of molybdenum; for $x > 0.50$ the bands

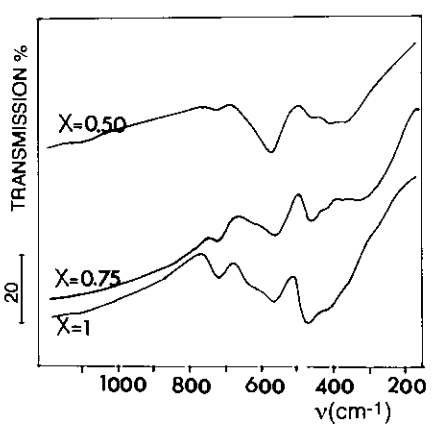

FIG. 3. FT-IR spectra of B samples for $0.50 < x < 1$.

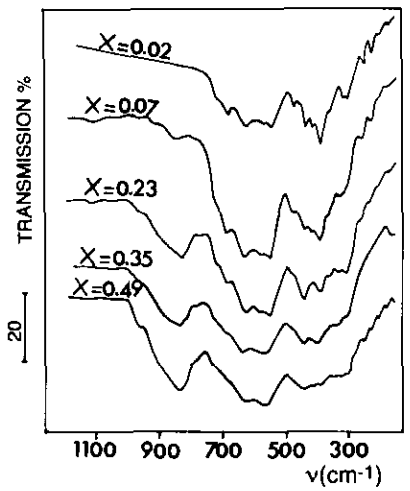

FIG. 4. FT-IR spectra of A samples oxidized in cation-deficient spinels at 530°C for 4 hr.

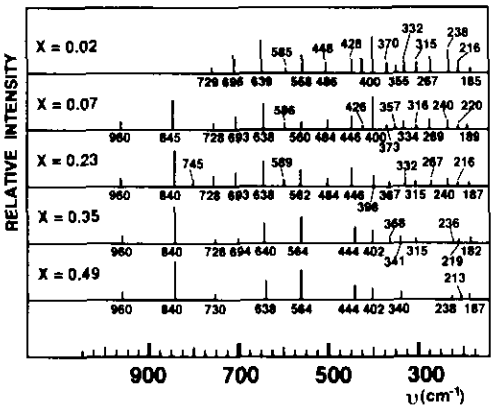

FIG. 5. Vibrational behavior of cation-deficient spinels for A samples.

could be discerned very clearly. It is also seen (Fig. 1 and 3) that besides the main band at 580 cm^{-1}, there is a band at 726 cm^{-1} whose intensity increases with molybdenum content. At higher frequencies and for certain compositions some weaker bands (indicated by arrows) are detected for samples A (Fig. 1) but are absent from samples B (Fig. 3).

Cation-Deficient Spinels and Transformation Products

Figure 4 shows the profile of the IR spectra and Fig. 5, the vibrational behavior of cation-deficent spinels obtained after oxidation for 4 hr at 530°C of substituted submicrometer magnetites. Over the range 150–750 cm^{-1} and for $x < 0.10$, three strong bands occurred at 400, 558, and 638 cm^{-1} with roughly 10 bands of relatively weak intensity. For compositions $x > 0.10$, the spectrum exhibits a number of different bands but shows considerable variation in absorption frequencies and intensities, particularly over the range 250–500 cm^{-1}. In the higher frequency absorption region, two other bands are found at 840 and 960 cm^{-1} whose intensity increases with molybdenum concentration.

After heating at higher temperatures (e.g., at 650°C for 4 hr), X-ray diffraction analysis has shown that the cation-deficient spinels are converted into iron III molybdate $Fe_2(MoO_4)_3$ and α-Fe_2O_3 (*1*). Following this transformation, the IR spectrum (Fig. 6,

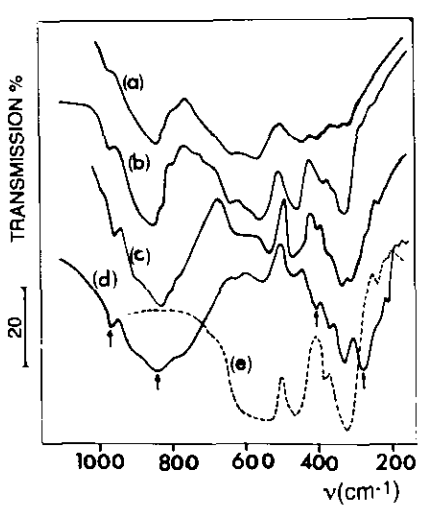

FIG. 6. FT-IR spectra of (a) sample A with $x = 0.49$ oxidized in cation-deficient spinel at 530°C for 4 hr, (b) sample A with $x = 0.49$ after transformation, (c) sample B with $x = 1$ after transformation, (d) pure $Fe_2(MoO_4)_3$, (e) pure α-Fe_2O_3.

curves b and c) always exhibits two absorption bands at 840 and 960 cm^{-1}, and new bands appear in the 700–300 cm^{-1} region. These two bands are also observed, without significant modification, for pure $Fe_2(MoO_4)_3$ (Fig. 6, curve d), and bands in similar positions were detected in the spectrum before transformation (Fig. 6, curve a).

Discussion

Initial Phases

For the IR absorption spectrum study of the solid solutions $(M, Fe)_3O_4$, Ishii and Nakahira (*7*) calculated the optically active lattice vibrations of Fe_3O_4. They assigned the band at 570 cm^{-1} to the υ_1 (T_{1u}) mode, which is the Fe-O stretching mode of the octahedral and tetrahedral sites; they assigned the band at 370 cm^{-1} to the υ_2 (T_{1u}) mode, which is an Fe-O stretching mode of the octahedral sites. The bands related to the υ_3 (T_{1u}) and υ_4 (T_{1u}) modes were assigned by these authors to the motion of Fe^{2+} ions on *A* sites against those of *B* sites, and to an O–Fe–O bending mode of the *A* and *B* sites, respectively. These bands, which are expected to be weak, have not been observed down to 50 cm^{-1}.

From Fig. 2 it can be seen that the positions of the bands υ_1 and υ_2 change slightly with x, due to the slight variation in the $Fe^{3+} - O^{2-}$ complexes with the increase of molybdenum content. In addition to the Fe^{3+} ions on *B* sites, Mo^{3+} ions are also present. With an increase of $Mo^{3+} - O^{2-}$ complexes an increase in the intensity of the two small bands at about 440 cm^{-1} is expected; this is confirmed by the results. Thus, these bands can be assigned to the $Mo^{3+} - O^{2-}$ octahedral complexes. This implies that with the increase of the $Mo^{3+} - O^{2-}$ complexes, the band at 380 cm^{-1}; which is an Fe–O stretching mode of octahedral sites, should disappear at higher molybdenum content.

The band at 726 cm^{-1} should be assigned to a vibration of the octahedral groups because of the presence of the highest valency cation (*8*) (Mo^{4+} cations on B sites) as shown by the cation distribution (1). This band cannot be attributed to the small amount of Mo^{4+} ions on *A* sites detected only for samples *A*. Thus, this band has been assigned to MoO_6 octahedra. For iron molybdenum (IV) oxide, $Fe_2Mo_3O_8$, whose Mo^{4+} ions are also in octahedral coordination with oxygen (*9*), a strong absorption band assigned to MoO_6 octahedra occurs at 727 cm^{-1}.

Cation-Deficient Spinels and Transformation Products

The three strong bands observed at 398, 560, and 630 cm^{-1} are assumed to be due to the stretching vibration υ of the Fe–O bonds. The assignment of the 398 and 560 cm^{-1} bands to the Fe–O stretch is consistent with their assignment for starting samples. Based only on intensity considerations the 638 and probably 446 cm^{-1} bands should also be those of υFe–O. The relatively weak intensities of the bands at 216, 240, 267, 315, 332, 370, 400, 428, 446, 486, 585, and 696 cm^{-1}, assumed to be due to the bending vibrations of the O–Fe–O bonds. However, some of the frequencies could be due to stretching vibrations of the spinel structure arising from the lower symmetry resulting from ordered vacancies on *B* sites (*10*). We have performed a systematic study of the ordered forms of cation-deficient spinels, resulting in a lowering of the overall symmetry, which leads to an increasing number of IR active vibrations (*11–13*). One of the first reported examples of the influence of cation ordering on the IR spectrum is the cation deficient spinels $(Fe^{3+})_A(Fe^{3+}_{(5-8y)/3}M^{3+}_{8y/3}\square_{1/3})_BO^{2-}_4$ ($0 < y < \frac{2}{3}$ and $M = Al^{3+}$, Cr^{3+}) (*11*) in which 1 : 5 ordering between vacancies and cations on *B* sites occurs for low y values. For molybdenum substituted

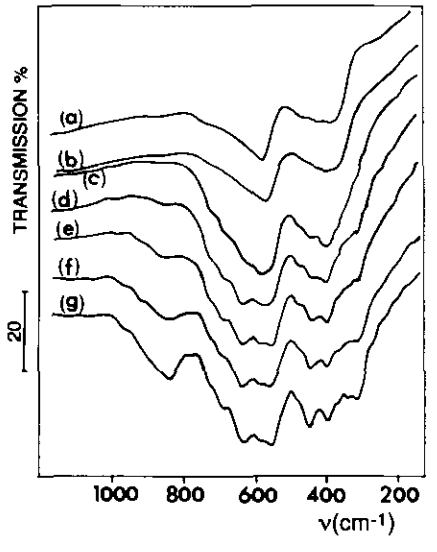

FIG. 7. FT-IR spectra of sample A with $x = 0.23$ oxidized under isothermal conditions for 4 hr at (a) 30°C, (b) 100°C, (c) 155°C, (d) 200°C, (e) 260°C, (f) 390°C, and (g) 500°C.

γ-Fe_2O_3 samples, the extended formula can be written as (3):

$$(Mo^{6+}_{8x/3(3+x)}\,Fe^{3+}_{(9-5)x/3(3+x)})_A\,(Fe^{3+}_{(5-x)/(3+x)}\,\square_{(1+3x)/(3+x)})_B\,O_4^{2-} \quad (2)$$

For $x < 0.10$, e.g., $x = 0.07$, the $\square/Fe^{3+}$ ratio in B sites was 0.24 and changed little compared to γ-Fe_2O_3 ($\square/Fe^{3+} = 0.20$) of the cation distribution $(Fe^{3+})_A(Fe^{3+}_{5/3}\,\square_{1/3})_B O_4^{2-}$, which would explain the preservation of ordering.

At higher molybdenum substitution content, e.g., $x = 0.23$, the $\square$, Fe^{3+} ratio was 0.34; the presence of numerous bands (Fig. 7, curve g) may indicate an ionic ordering 1 : 3 on the B sites. At certain oxidation temperatures, the local symmetry did change, as observed for the sample with $x = 0.23$ heated in isothermal conditions at various temperatures (Fig. 7). This implies that the number of vacancies for a given substitution content can influence the ordering. For this purpose, if we select the oxidation temperature (e.g., 200°C) in order to oxidize only the octahedral Fe^{2+} ions thereby to preserve the oxidation of other cations (Fig. 7, curve d), the number of vacancies decreases according to the formula:

$$(Mo^{4+\,\text{ou}\,5+}_{8\gamma x/y}\,Fe^{3+}_{(9(1-\beta)+(\alpha-8\gamma)x)}\,Fe^{2+}_{8\beta/y})_A \cdots (Mo^{4+}_{8(\alpha-\gamma)x/y}\,Mo^{3+}_{8(1-\alpha)x/y}\,Fe^{3+}_{(15+\beta+(8\gamma-\alpha-8)x)/y}\,\square_{3(1-b+a)x/y})_B\,O_4^{2-}, \quad (3)$$

and the $\square/$ cation ratio at this temperature again approaches 0.20. However, because Mo^{3+} and Mo^{4+} have a strong preference for the octahedral environment, the presence of some kinds of cations at B sites will broaden the absorption bands. From the IR spectra of oxidized samples with $x > 0.30$ (Fig. 4), it is seen that the absorption bands over the range 200–700 cm^{-1}, are not so distinct as those of the low substitution content. The absence of ordering can be explained by the large number of vacancies.

Figures 4 and 7, show two other bands at 840 and 960 cm^{-1} whose intensity increases with molybdenum concentration and oxidation temperature. These bands may be associated with the presence of Mo^{6+} ions at A sites. They are attributed to isolated MoO_4 tetrahedra. In $MoAg_2O_4$, in $MoNa_2O_4$ of spinel structure, or in most of the molybdates ($BaMoO_4$, $CaMoO_4$, $PbMoO_4$) in which the molybdenum is tetrahedrally coordinated by oxygen, the strong band at 840 cm^{-1} is also assigned to MoO_4 tetrahedra (*14, 15*). Moreover, the similarity of the spectra to those of $Fe_2(MoO_4)_3$ (Fig. 6, curve d) shows that the high frequency band may be assigned to a vibration of the symmetric stretch of MoO_4 tetrahedral groups. This confirms that oxygen is 4-fold coordinated around the molybdenum. In all cases, the symmetry site is T_d and the observed frequency values (indicated by arrows in Fig. 6) for the two antisymmetrical stretching (960 and 840 cm^{-1}) and the two bending (413 and 287 cm^{-1}) vibrations are consistent with this symmetry (*16–18*). The remaining bands at 542, 470, 377, 339, 238, and 212 cm^{-1} and the weak shoulder at about 619

cm^{-1} must be related to α-Fe_2O_3 bands in comparison with pure α-Fe_2O_3 (Fig. 6, curve e). This analogy confirms that in this molybdate the oxygen atoms are octahedrally coordinated with the iron atoms. In both samples *A* and *B*, the presence of Mo^{6+} ions at *A* sites for cation deficient spinels requires that the extraction of three electrons to a Mo^{3+} ion to produce Mo^{6+} ions during the oxidation. This requires a transfer of Mo^{6+} ions from the *B* sites to the *A* sites, with a concomitant migration of Fe^{3+} ions from *A* to *B* sites. Moreover, from the IR spectra of Figs. 4 and 7, it can be seen that at temperatures higher than 450°C, the absorption band at 726 cm^{-1} has disappeared, indicating that the Mo^{4+} ions have been oxidized, as proved by thermogravimetric analysis.

The same spectrum was observed for ground samples *B* oxidized in isothermal conditions for 4 hr as for unground samples. Here the experimental conditions were changed; the temperature increased at a linear rate of 2.5°C min^{-1}. The 840 and 960 bands disappeared while new bands at 788, 861, and 915 cm^{-1} appeared (Fig. 8). In this particular case, we used the DTG (*2*) to prove that a sizeable amount of Fe_B^{2+} ions is not oxidized, although we observe a complete oxidation of Mo_B^{3+} ions. On the other hand, for long reaction times, the Fe_B^{2+} ions of the sample A and those of the ground samples B are totally oxidized, whereas only a small amount of Mo_B^{3+} ions is oxidized. The three bands at 788, 861, and 915 cm^{-1} also occur for samples A oxidized under certain conditions if Fe_B^{2+} and Mo_B^{6+} ions are present together. This happens, for example, if the samples are oxidized at 290°C for various short reaction times (Fig. 9), or if initially oxidized samples in cation-deficient spinels are reduced in H_2 in order to restore a part of the Fe^{2+} ions (Fig. 10). By analogy with molybdates of Co(II) (*19*) and Fe(II) (*20*), we believe that under these treatment conditions, Mo^{6+} is located in a *B* site which is distorted by contraction of the O^{2-} ions around the cations with highest charges.

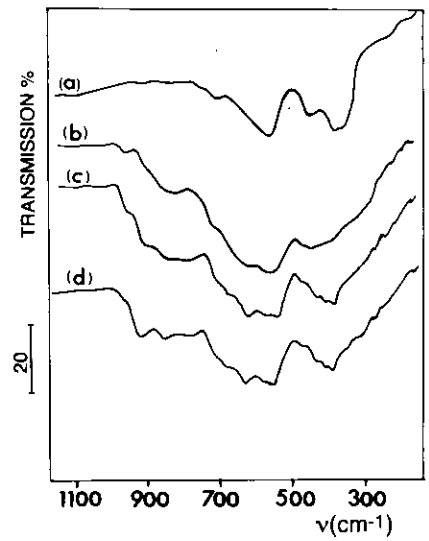

FIG. 9. FT-IR spectra of sample A with $x = 0.49$ (a) before oxidation and oxidized at 290°C for (b) 30 min, (c) 15 min, and (d) 3 min.

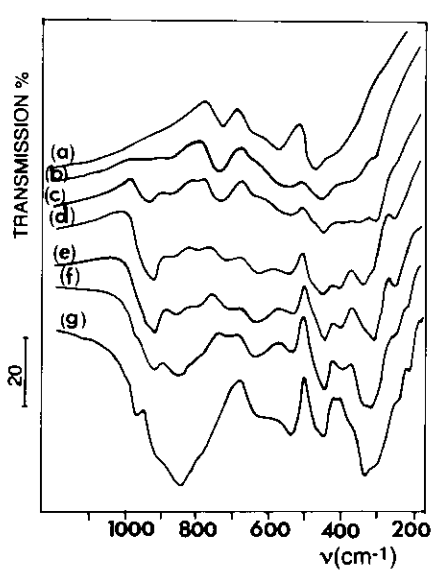

FIG. 8. Evolution of FT-IR spectra of sample B with $x = 1$ (a) before oxidation and oxidized under nonisothermal conditions (2.5°C min^{-1}) at (b) 500°C, (c) 528°C, (d) 590°C, (e) 639°C, (f) 663°C, and (g) 700°C.

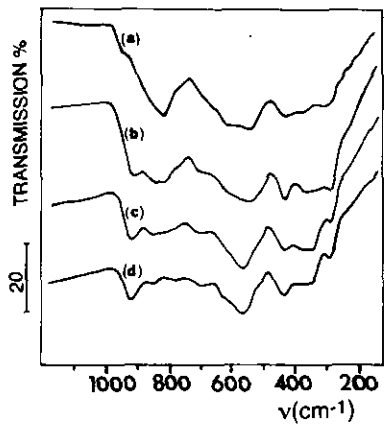

FIG. 10. FT-IR spectra of cation-deficient spinel with $x = 0.49$ showing the evolution of the spectra (a) before reduction and after partial reduction for different percentages of Fe^{2+} ions on *B* sites: (b) 50%, (c) 80%, and (d) 100%.

This is consistent with the bands at 980, 860, and 790 cm^{-1} observed for b-$FeMoO_4$ or b · $CoMoO_4$, and is typical of a distorded octahedral coordination of Mo. A structural analysis has shown that for these molybdates the oxygens are six-fold co-ordinated around molybdenum in two distorted octahedral arrangements, with a wide range of Mo–O distances between 0.172 and 0.233 nm. Moreover, Fig. 10 shows that the percentage of Mo^{6+} ions on *B* sites depends on the fraction of restored Fe^{2+} ions. Consequently, the presence of divalent cations on *B* sites stabilizes the octahedral coordination of Mo^{6+} ions. This is in agreement with the b · $CoMoO_4$ and b-$FeMoO_4$ structure for which the Co^{2+} and Fe^{2+} cations are also in octahedral sites. The very weak bands observed at high frequencies in the case of the initial submicrometer samples are identified as those characteristic of the Mo^{6+} in *B* sites and prove that the Mo^{3+} ions are oxidized at room temperature inside a small thickness.

In conclusion, this work has demonstrated very interesting cationic migration and ionic ordering undergone by molybdenum substituted magnetites oxidized in cation-deficient spinels. The comparative IR study of the oxidation products prepared by two different methods established that the Mo^{6+} ions can be present both in isolated MoO_4 tetrahedral and in distorted MoO_6 octahedra. For submicrometer cation deficient spinels with Mo^{6+} ions in tetrahedral sites, the results of our investigation suggest an ordered distribution of cations and vacancies at octahedral sites, in conformity with an increasing number of IR active vibrations resulting from an $\square/Fe^{3+} = \frac{1}{5}$ or $\square/Fe^{3+} = \frac{1}{3}$ ratio. The absence of a 1:2 order for oxidized sample with $x = 0.49$ can be explained by the vacancy migration on tetrahedral sites. With Mo^{6+} ions in octahedral sites the ordering process is prevented by the presence of some kinds of cations at these sites.

References

1. L. BOUET, P. TAILHADES, A. ROUSSET, AND B. GILLOT, *C.R. Séances Acad. Sci. Série 2*, **312,** 1507 (1991).
2. B. DOMENICHINI, B. GILLOT, AND P. TAILHADES, *Thermochim. Acta*, in press.
3. B. DOMENICHINI, B. GILLOT, P. TAILHADES, L. BOUET, AND A. ROUSSET, *Solid State Ionics*, in press.
4. M. GUPTA, S. KANETKAR, S. DATE, N. NIGAKEVAR, AND A. SINHA, *J. Phys. C* **12,** 2411 (1979).
5. A. RAMDANI, C. GLEITZER, G. GAVOILLE, A. K. CHEETHAM, AND J. B. GOODENOUGH, *J. Solid Stat. Chem.* **60,** 269 (1985).
6. M. R. PRAIRIE, S. SU, A. RENKEN, P. RUTERANA, AND P. A. BUFFAT, *Appl. Cataly.* **57,** 83 (1990).
7. M. ISHII AND M. NAKAHIRA, *Solid State Commun.* **11,** 209 (1972).
8. P. TARTE, A. RULMONT, M. LIEGEOIS-DUYCKAERS, R. CAHAY, AND J. M. WINARD, *Solid State Ionics*, **42,** 177 (1990).
9. G. B. ANSELL AND L. KATZ, *Acta Crystallogr.* **21,** 482 (1966).
10. D. M. FARRELL, Report IR 72-18, pp. 1–44, Mines Branch Investigation, Ottawa (1972).
11. B. GILLOT, J. F. FERRIOT, F. BOUTON, F. CHASSAGNEUX, AND A. ROUSSET, *J. Solid State Chem.* **21,** 375 (1977).

12. B. GILLOT AND F. BOUTON, *J. Solid State Chem.* **32,** 303 (1980).
13. B. GILLOT, *Mater. Chem. Phys.* **10,** 375 (1985).
14. G. M. CLARK AND W. P. DOYLE, *Spectrochim. Acta* **22,** 1441 (1966).
15. J. PREUDHOMME AND P. TARTE, *Spectrochim. Acta* **28,** 69 (1972).
16. J. A. CAMPBELL, *Spectrochim. Acta* **21,** 1333 (1965).
17. R. H. BUSEY AND O. L. KELLER, JR., *J. Chem. Phys.* **41,** 215 (1964).
18. J. DONOHUE AND W. SHAND, JR., *J. Am. Chem. Soc.* **69,** 222 (1947).
19. P. P. CORD, P. COURTINE, P. PANNETIER, AND J. GUILLERNET, *Spectrochim. Acta A* **28,** 1601 (1972).
20. F. TRIFIRO, G. CAPUTO, AND P. L. VILLA, J. *Less-Common Met.* **36,** 305 (1974)